The unique cytoarchitecture of human pancreatic islets has implications for islet cell function

Over Cabrera*, Dora M. Berman*, Norma S. Kenyon*, Camillo Ricordi*, Per-Olof Berggren*†‡, and Alejandro Caicedo*§

*Diabetes Research Institute, Miller School of Medicine, University of Miami, Miami, FL 33136; and †The Rolf Luft Center for Diabetes Research, Department of Molecular Medicine, Karolinska Institutet, SE-171 76 Stockholm, Sweden

Communicated by Rolf Luft, Karolinska Institute, Stockholm, Sweden, December 21, 2005 (received for review July 5, 2005)

The cytoarchitecture of human islets has been examined, focusing on cellular associations that provide the anatomical framework for paracrine interactions. By using confocal microscopy and multiple immunofluorescence, we found that, contrary to descriptions of prototypical islets in textbooks and in the literature, human islets did not show anatomical subdivisions. Insulin-immunoreactive β cells, glucagon-immunoreactive α cells, and somatostatin-containing δ cells were found scattered throughout the human islet. Human β cells were not clustered, and most (71%) showed associations with other endocrine cells, suggesting unique paracrine interactions in human islets. Human islets contained proportionally fewer β cells and more α cells than did mouse islets. In human islets, most β, α, and δ cells were aligned along blood vessels with no particular order or arrangement, indicating that islet microcirculation likely does not determine the order of paracrine interactions. We further investigated whether the unique human islet cytoarchitecture had functional implications. Applying imaging of cytoplasmic free Ca^{2+} concentration, $[Ca^{2+}]_i$, we found that β cell oscillatory activity was not coordinated throughout the human islet as it was in mouse islets. Furthermore, human islets responded with an increase in $[Ca^{2+}]_i$ when lowering the glucose concentration to 1 mM, which can be attributed to the large contribution of α cells to the islet composition. We conclude that the unique cellular arrangement of human islets has functional implications for islet cell function.

α cell | β cell | cytoplasmic free Ca^{2+} concentration | insulin | glucagon

In the last three decades, hundreds of individuals with type 1 diabetes mellitus have received allogeneic transplants of endocrine pancreas, the islets of Langerhans, to cure their chronic condition. In these patients, diabetes is reversed by transplanting cells capable of physiologically regulating insulin secretion. Determining the quality of islets obtained from cadaveric pancreata should be indispensable in this context. However, it is not known which physiological parameters correlate best with a fully functional islet capable of reversing diabetes after transplantation. There is a wealth of information about the physiology of rodent islets, but the biology of human islets remains poorly understood. As assays for determining islet quality are being developed by many laboratories in the field of islet transplantation, a reassessment of the structure and function of human islets is warranted.

The islets of Langerhans are small organs located in the pancreas that are crucial for glucose homeostasis. Islets typically consist of four types of secretory endocrine cells, namely, the insulin-containing β cells, the glucagon-containing α cells, the somatostatin-containing δ cells, and the pancreatic polypeptide-producing (PP) cells. In rodent islets, the vastly predominating β cells are clustered in the core of a generally round islet, surrounded by a mantle of α, δ, and PP cells. Thus, in rodent islets, there is a clear segregation of cell types to different regions of the islet, suggesting that there are anatomical subdivisions in the islet (1). Although this is the prevailing description found in textbooks in endocrinology (e.g., refs. 2 and 3), large interspecies variabilities in cell composition and structure of the islet have been reported (4).

Detailed quantitative studies assessing the cell composition of human islets are sparse (5–7). These studies have reported that islets are composed of $\approx$70% β cells, 20% α cells, $<$10% δ cells, and $<$5% PP cells. More recent studies, however, have provided lower numbers of β cells and higher numbers of α cells (8–10). More importantly, no studies have addressed how the different cell types are distributed within human islets and how they relate to the islet's microcirculation and islet function. Although mentioned in the literature (1, 11), the notion that human or monkey islets lack the organization seen in rodent islets has largely been dismissed.

To address this question, we have examined the cell composition of islets in human pancreatic sections by using confocal microscopy and multiple immunofluorescence labeling. We enumerated the proportional contribution of the different cell types to the islet and the associations among endocrine cells and between endocrine cells and blood vessels. We were particularly interested in comparing the cytoarchitectural pattern of the human islet with that of the mouse islet, which has been considered to be a prototypical islet. In addition, we conducted imaging studies of cytoplasmic free Ca^{2+} concentration, $[Ca^{2+}]_i$, to establish whether there were functional differences among mouse, monkey, and human islets. Our results show striking species differences with regard to both cytoarchitecture and function and emphasize that human islet structure and function need to be reevaluated.

Results

As a first step toward a characterization of human islets of Langerhans, we investigated whether human islets belong to the prototypical islet type described in many textbooks. We compared the cellular composition of human islets to that of the islets of three other mammalian species by using confocal microscopy and multiple immunofluorescence. The presence of cells expressing insulin, glucagon, and somatostatin was detected in sections of human, monkey, pig, and mouse pancreata (Fig. 1). In the islets of all species examined, insulin-expressing cells were the most abundant. However, mouse islets were unique in that they were mainly composed of insulin-expressing cells clustered in the core of the islet (Fig. 1*C*). The few glucagon-immunoreactive cells in mouse islets were localized to the periphery of the islet (Fig. 1*C*). In human and monkey islets, by contrast, glucagon-containing cells were numerous and were found scattered throughout the islet (Fig. 1 *A* and *B*). Soma-

Conflict of interest statement: No conflicts declared.

Abbreviations: $[Ca^{2+}]_i$, cytoplasmic free calcium concentration; PP, pancreatic polypeptide.

‡To whom correspondence may be addressed at: The Rolf Luft Center for Diabetes Research, Department of Molecular Medicine, Karolinska Institutet, Karolinska University Hospital Solna, SE-171 76 Stockholm, Sweden. E-mail: per-olof.berggren@molmed.ki.se.

§To whom correspondence may be addressed at: Diabetes Research Institute, Miller School of Medicine, University of Miami, 1450 NW 10th Avenue, Miami, FL 33136. E-mail: acaicedo@med.miami.edu.

www.pnas.org/cgi/doi/10.1073/pnas.0510790103

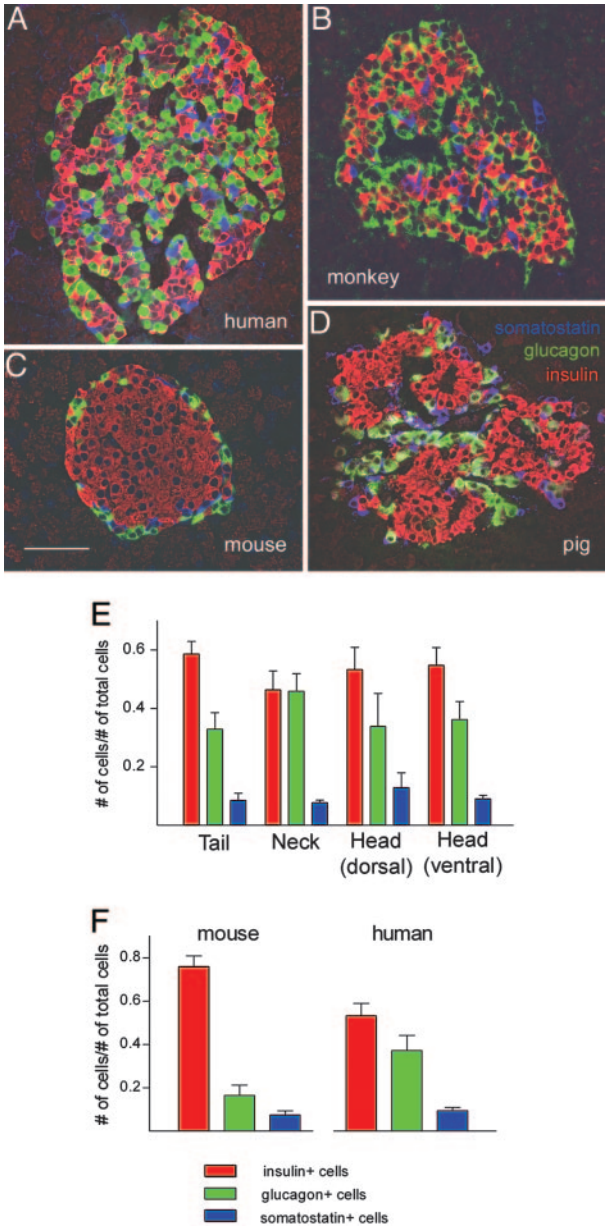

Fig. 1. Islets of Langerhans show striking interspecies differences. (*A–D*) Confocal micrographs (1-μm optical sections), showing representative immunostained pancreatic sections containing islets of Langerhans from human (*A*), monkey (*B*), mouse (*C*), and pig (*D*). Insulin-immunoreactive (red), glucagon-immunoreactive (green), and somatostatin-immunoreactive (blue) cells were all found randomly distributed in human and monkey islets. By contrast, insulin-containing cells were located in the core, and glucagon- and somatostatin-containing cells in the mantle of mouse islets. Pig islets seemed to be formed of smaller units (three, in this case) showing a core–mantle organization. (Scale bar, 50 μm). (*E*) Quantitative enumeration of the contribution of insulin-, glucagon-, and somatostatin-immunoreactive cells to the composition of islets in four different regions of the human pancreas ($n = 5$ subjects; mean $\pm$ SEM). (*F*) Comparison of the cell composition of human islets with that of mouse islets. Human islets had more glucagon-immunoreactive cells and fewer insulin-immunoreactive cells ($n = 3$ mice and 5 humans; mean $\pm$ SEM).

tostatin- and PP-expressing cells constituted a minority in islets from all species. In mouse islets, but not in those of the other species, somatostatin-immunoreactive cells were preferentially located in the periphery (Fig. 1*C*). Pig islets seemed to be composed of several smaller subunits that resembled mouse islets (Fig. 1*D*). Our results confirmed previous studies on the

Table 1. Homotypic and heterotypic contacts of cells within the islet

	Mouse		Human	
Cell type	Heterotypic, %	Homotypic, %	Heterotypic, %	Homotypic, %
β cells	28 $\pm$ 6	71 $\pm$ 4	71 $\pm$ 5	29 $\pm$ 5
α cells	98 $\pm$ 1	2 $\pm$ 1	90 $\pm$ 3	10 $\pm$ 3

composition of mouse islets but pointed to striking interspecies differences in the structure of islets of Langerhans, in particular between primate and rodent islets (see also ref. 4).

There are few detailed studies on the cellular composition of human islets (5–7, 10). Using our approach (see above), we decided to enumerate the relative contribution of cells containing insulin, glucagon, and somatostatin to the composition of islets located in four different regions of the human pancreas. Islets in the four regions examined had a similar composition, although the neck of the pancreas showed islets with a somewhat higher proportion of glucagon-immunoreactive cells (Fig. 1*E*). Depending on the region, insulin-containing cells contributed between 48% and 59% of the total cell population, glucagon-containing cells between 33% and 46%, and somatostatin-containing cells between 8% and 12%. There was variability in the cell composition between islets within each region; some islets were mainly composed of insulin-immunoreactive cells (range, 32–77%) and other islets mainly of glucagon-immunoreactive cells (range, 15–50%). The average cell composition of human islets differed from that of mouse islets (Fig. 1*F*). The proportion of insulin-containing cells was higher in mouse than in human islets (77% versus 55%; ANOVA, followed by Bonferroni multiple comparisons test, $P < 0.05$), and the proportion of glucagon-containing cells was lower (18% versus 38%; $P < 0.05$). Because we used the same approach to quantify the different cell types in both mouse and human islets, we conclude that our results reflect major differences in the cell composition between the two species.

To estimate the degree of clustering or segregation of cell types within the islet, we further enumerated the proportion of insulin- and glucagon-containing cells exclusively apposed to cells of the same type (homotypic associations) versus the proportion of cells closely apposed to cells of other cell types (heterotypic associations). In mouse islets, 71% of the insulin-containing cells showed exclusively homotypic associations, whereas, in human islets, only 29% showed these associations (Table 1; ANOVA, followed by Bonferroni multiple compari-

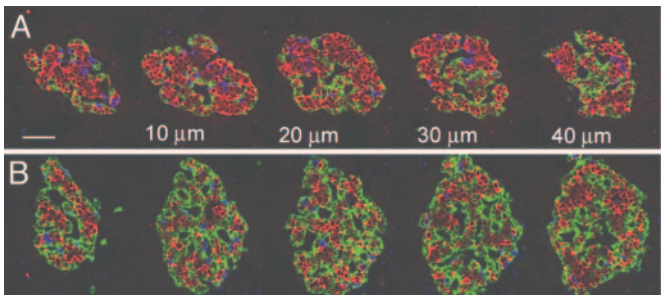

Fig. 2. Confocal micrographs (1-μm optical sections) of two series of five consecutive human pancreatic sections (10 μm apart), showing that the cytoarchitecture did not change within a given islet. Similar proportions of insulin- (red), glucagon- (green), and somatostatin- (blue) immunoreactive cells could be seen in all sections. Two islets are shown; the equatorial plane for *A* is shown third from the left and, for *B*, fourth from the left. (Scale bar, 50 μm.)

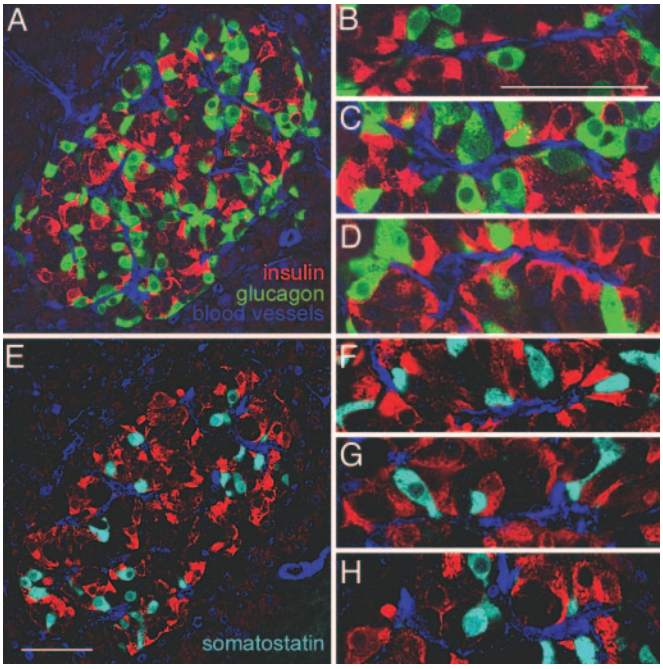

Fig. 3. Endocrine cells in human islets were closely but randomly associated with vascular cells. Most insulin- (red), glucagon- (green), and somatostatin- (cyan) immunoreactive cells were in close proximity to vascular cells immunoreactive for both smooth muscle cell actin (vascular smooth muscle cells, blue) and CD34 (endothelial cells, blue). Note that many blood vessels were cut along their main axis, allowing for inspection of long tracts (*B–D* and *F–H*). Endocrine cells were aligned along the blood vessels in a random order; insulin-immunoreactive cells were bordered on both sides by glucagon- (*B–D*) or somatostatin- (*F–H*) immunoreactive cells and vice versa. Cells from different cell types were seen facing each other across the lumen of the blood vessel. The image shown in *C* is a higher magnification of a region in *A*; the image shown in *H* is a higher magnification of a region in *E*. (Scale bars, 50 μm.)

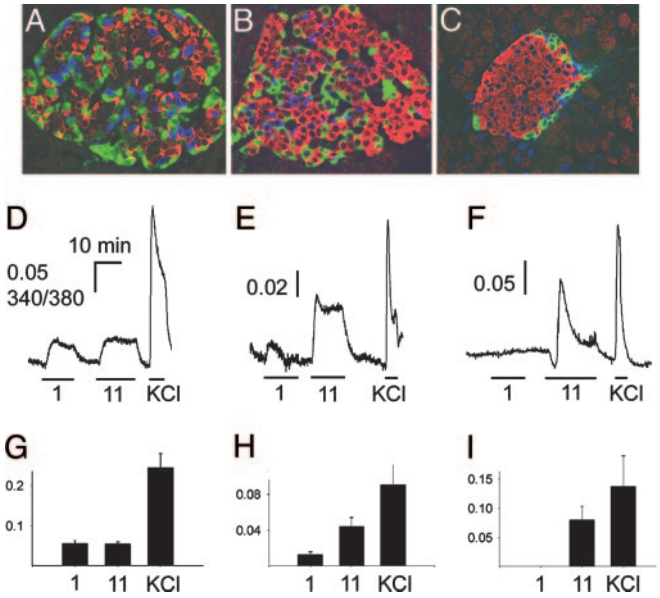

Fig. 4. Human, monkey, and mouse islets showed functional differences that correlated with structural differences. Different contributions of glucagon-immunoreactive cells were seen for the three species; in human islets (*A*), the contribution was ≈38%, in monkey islets (*B*), ≈25%, and, in mouse islets (*C*), ≈18%. (Scale bar, 50 μm.) $[Ca^{2+}]_i$ responses (Fura 2-AM) elicited by low glucose (1 mM, 1), high glucose (11 mM, 11), and high KCl (30 mM, KCl) showed that human (*D*) and monkey islets (*E*), but not mouse islets (*F*) responded to low glucose. Bars under the traces indicate the duration of the stimulus. The peak amplitudes of these responses were quantified for human (*G*), monkey (*H*), and mouse (*I*) islets ($n \geq 10$ islets).

sons test, $P < 0.001$). Conversely, 71% of the insulin-containing cells in human islets showed associations with other cell types. In both species, >90% of the glucagon-containing cells were in close proximity to cells of other cell types ($P > 0.05$). These results demonstrate that insulin-containing cells are more clustered in mouse islets than in human islets and that human insulin-containing cells intermingle with other cell types within the islet. To rule out the possibility that our results on human islets were due to biased sampling of islets, we examined serial sections of the same islet. We found that all sections from the same islet showed a similar cell composition and cytoarchitecture, independent of whether the sections were from the pole or equatorial regions of the islet (Fig. 2).

In contrast to the mouse islet, insulin-, glucagon-, and somatostatin-containing cells were found distributed throughout the human islet. Because endocrine cells are generally associated with blood vessels, we investigated whether this apparently random cellular organization reflected the vascularization pattern in human islets. We found that most of the cells, irrespective of cell type, were located close to islet blood vessels (Fig. 3). Eighty-six percent of the glucagon-immunoreactive and 77% of the insulin-immunoreactive cells were closely apposed to immunostained vascular endothelial and smooth muscle cells. The different cell types were aligned along the vessels with no particular sequence, i.e., glucagon- or somatostatin-immunoreactive cells were seen on both sides of insulin-immunoreactive cells and vice versa (Fig. 3). We were not able to determine whether cells were upstream or downstream of each other. The random arrangement, however, was independent of whether we examined the sequence from one side or the other (Fig. 3). Furthermore, many insulin-immunoreactive cells were seen facing glucagon- or somatostatin-immunoreactive cells across the blood vessel lumen (Fig. 3).

To examine whether the morphological differences between mouse and human islets had functional correlates, we performed imaging experiments of $[Ca^{2+}]_i$ in whole islets. Human, monkey, and mouse islets loaded with the Ca^{2+} indicator Fura-2 showed an increase in $[Ca^{2+}]_i$ in response to an elevation of the extracellular glucose concentration (11 mM; Fig. 4). Furthermore, human and monkey islets responded with an increase in $[Ca^{2+}]_i$ when the extracellular glucose concentration was decreased from 3 mM to 1 mM (Fig. 4 *D*, *E*, *G*, and *H*). These responses were absent in mouse islets (Fig. 4 *F* and *I*). By using $[Ca^{2+}]_i$ imaging in dissociated human and monkey islet cells, we found that reducing the glucose concentration elicited $[Ca^{2+}]_i$ transients in a subset (≈20%) of islet cells that was glucagon-immunoreactive (data not shown) (for activation of α cells at low glucose concentrations, see also ref. 12). We conclude that $[Ca^{2+}]_i$ responses to low glucose levels were detectable in whole human and monkey islets because of the large contribution of α cells to the islets in these species.

Do the differences in cellular organization have other consequences for islet physiology? It has been widely reported for rodent islets that the activity of β cells, in particular their oscillatory behavior, is synchronized throughout the islet, thus forming a functional syncytium (e.g., refs. 13 and 14). We found that mouse islets showed oscillations in $[Ca^{2+}]_i$ in their response to prolonged glucose elevations (11 mM; Fig. 5*A*; $n = 6$). By contrast, this type of response could not be elicited in human or monkey islets (Fig. 5*B*; $n \geq 70$ islets from ≥10 preparations for human and monkey islets). When smaller regions were examined within the whole islet, however, oscillatory responses in $[Ca^{2+}]_i$ could also be discerned in human or monkey islets (Fig. 5 *C* and

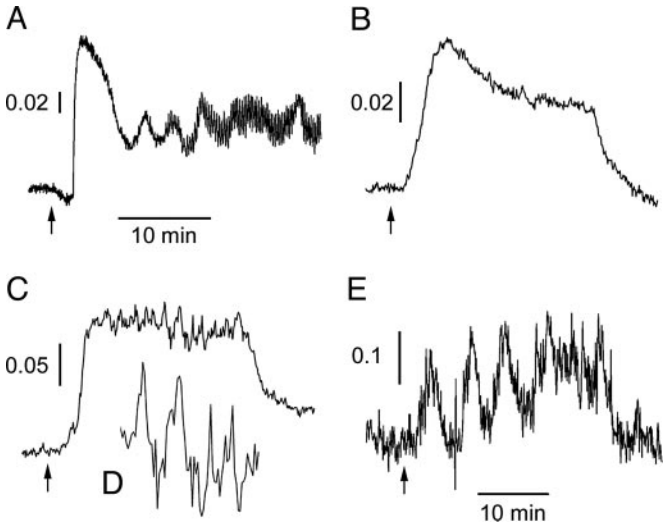

Fig. 5. $[Ca^{2+}]_i$ responses of β cells were not synchronized in human islets. Oscillations in the $[Ca^{2+}]_i$ response to high glucose (11 mM) could be readily detected when recording from whole mouse islets (*A*) ($n = 6$ islets). By contrast, oscillatory responses could not be seen when recording from whole human islets (*B*) (representative trace of ≥70 islets from 10 preparations). Oscillations in the $[Ca^{2+}]_i$ response were discernible only in small areas of the islet that corresponded in size to single cells or small groups of cells (*C*). (*D*) A magnification of *C*. Isolated human β cells showed oscillatory $[Ca^{2+}]_i$ responses to high glucose concentrations (*E*) (11 mM; $n = 48$ of 66 cells from four preparations). The time scale in *A* also applies to *B* and *C*. Arrows indicate the time point when the bath solution was switched from 3 mM to 11 mM glucose.

D). Isolated human or monkey β cells also showed oscillatory responses to elevated glucose concentrations (Fig. 5*E*; 48 of 66 cells from four human preparations and 18 of 26 cells from five monkey preparations). These results suggest that, whereas individual β cells display an oscillatory response, these oscillations are not synchronized throughout the human or monkey islet and become neutralized by the out-of-synch activity from other islet regions. In human and monkey islets, β cell activity seems to be discontinuous, consistent with our morphological results showing that β cells in human and monkey islets are not clustered as they are in mouse islets.

Discussion

This study has revealed five findings relevant to the biology of human islets of Langerhans: (*i*) human islets contained proportionally fewer β cells and more α cells than mouse islets, the prototypical islets described in the literature; (*ii*) β cells intermingled with α and δ cells throughout the human islet; (*iii*) all endocrine cell types were closely associated with the islet's microcirculation; (*iv*) there was no particular order in the alignment of endocrine cells along the blood vessels; and (*v*) human islets have a distinct physiology that is consistent with the morphological findings.

The cellular composition of human islets described in our study is consistent with studies showing that human islets are composed of ≈60% β cells and ≈30% α cells (8–10, 15). However, islet descriptions in endocrinology textbooks (e.g., ref. 3) reflect results from other studies that have reported a cell composition similar to that of mouse islets, in which >70% of the cells are β cells, and <20% are α cells (5, 6). Cell numbers may inevitably differ between studies because cell composition varies strongly from islet to islet and from subject to subject (see refs. 5 and 10). In addition, the different immunohistochemical methods and quantification approaches used in the different studies may produce discrepant results. Nevertheless, we are confident that our technical approach yielded an accurate estimate of the cell proportions in the islet. By using confocal microscopy and multiple immunofluorescence to enumerate the proportional contribution of the different cell types in one and the same section, we have avoided the potential inaccuracies of counting cells in consecutive sections. Our immunohistochemical data are in line with results of recent reports using laser scanning confocal microscopy on whole isolated islets (10) and laser scanning cytometry on dispersed islet cells (16). Finally, the cell composition of mouse islets described in our study is consistent with that reported in the literature (e.g., refs. 17–19). The conclusion that human islet composition differs quantitatively from that of mouse islets thus seems inescapable. As discussed below, the relative contributions of the different endocrine cells to the human islet, in particular the larger proportion of α cells, likely have an impact on islet function.

The islets of the mammalian classes examined in this study had very distinct and unique cytoarchitectures (for a comparative study, see also ref. 4), suggesting that a prototypical mammalian islet type may not exist. The wide species variability in islet cell composition and topography might reflect evolutionary adaptations to different dietary habits or other environmental constraints. Additional comparative studies are needed to address these hypotheses. Nevertheless, the prevailing view is that there is a common mammalian scheme in islet architecture. Human islets have been considered to have a modified core–mantle structure. In this view, β cells are contiguous and arranged either into smaller clusters surrounded by non-β cells or along invaginations of the exterior surface of the islet (20, 21). Our results, however, indicate that human islets do not show obvious subdivisions. There was no clustering of β cells, and β cells intermingled freely with other endocrine cells throughout the islet. β, α, and δ cells had equivalent and random access to blood vessels within the islet, ruling out the possibility that the different endocrine cells are organized in layers around blood vessels.

Our results further indicate that cellular interactions in the islet may not be determined by the direction of blood flow (22, 23). It has been proposed, on the one hand, that the blood first flows through β cell regions and then through non-β cell regions. On the other hand, authors have suggested that non-β cell regions are perfused before β cell regions (for a review, see ref. 24). These models hold that the direction of blood flow in the islet establishes a signaling order, where one particular endocrine cell influences the other endocrine cells. Common to these models is the assumption that there is specific localization of endocrine cells in the islet (e.g., a mantle-core pattern). However, we found no evidence for subdivisions in human islets, and all endocrine cells examined were randomly associated with blood vessels. Thus, an anatomical basis for an order in paracrine signaling as determined by the direction of blood flow likely does not exist for human islets. Our results support a model in which there is no set order of islet perfusion and in which any given cell type can influence other cell types, including its own cell type (24).

The unique cellular topography of human islets had measurable consequences for islet function. Our $[Ca^{2+}]_i$ recordings from whole human islets did not show the typical oscillatory patterns described for rodent islets (13, 14). In rodent islets, β cells are clustered, and their oscillations in membrane potential and $[Ca^{2+}]_i$ in response to high glucose concentrations are coordinated. As a result, the whole islet displays a synchronous oscillatory response that may constitute the molecular basis for the typical pulsatility in insulin release. Although we were able to measure oscillatory $[Ca^{2+}]_i$ responses in individual β cells or in distinct regions within the islet, β cell activity in terms of $[Ca^{2+}]_i$ oscillations was not synchronized in human islets, suggesting that human β cells are functionally segregated, which is in line with our anatomical findings showing that they are not clustered. Interestingly, mice that lack connexin 36 have islets

that do not display regular $[Ca^{2+}]_i$ oscillations, because β cell synchronization is lost (25). In these mice, high glucose concentrations elicit $[Ca^{2+}]_i$ responses in whole islets that resemble those of human islets. An important functional consequence is that islets from these mice lose the ability to release insulin in a pulsatile fashion. How the unique structural and functional features of human islets affect insulin release remains to be determined.

Our results also demonstrate the importance of the relative contributions of the different endocrine cells for islet function. Species differences in islet cell composition have functional consequences, as suggested by our results showing that human and monkey islets, but not mouse islets, respond with $[Ca^{2+}]_i$ increases to low glucose concentrations. α cells are believed to be activated by hypoglycemia, and individual α cells in mouse islets (26) and isolated human α cells (this study) show $[Ca^{2+}]_i$ responses to low glucose concentrations. In mouse islets, α cells represent a small fraction, and their responses are not likely to be detected at the level of the whole islet. By contrast, $[Ca^{2+}]_i$ responses to low glucose concentrations can be recorded from whole human and monkey islets because these islets have a large proportion of α cells, and their individual responses add to give a measurable signal. Given their large contribution to the islet and their close association with β cells, α cells may exert a stronger influence on the overall activity of the human islet than in rodent islets.

Taken together, our results have provided a picture of human islets that differs from that of prototypical islets described in textbooks. Our anatomical and functional data point to the uniqueness of human islets but also emphasize that human islet biology is still poorly understood. An arrangement in which most β cells contact other endocrine cells and vice versa predisposes human islets for strong paracrine interactions. This same arrangement may not allow β cell oscillatory activity to be coordinated throughout the islet. How human islet architecture affects cell-to-cell interactions that lead to regulated and concerted hormonal secretion remains to be determined.

Experimental Procedures

Human pancreata were obtained from multiorgan cadaveric donors ($n = 5$, age, 48 ± 7). Monkey islets were isolated from cynomolgus monkeys (*Macacca fascicularis;* $n = 3$) >4 years of age at the time of pancreas procurement. The pig pancreas was procured from the local slaughterhouse. Mice (C57BL/6; $n = 5$) were killed by exposure to a rising concentration of CO_2, followed by cervical dislocation. All experimental protocols using mice were approved by the University of Miami Care and Use Committee.

Immunohistochemistry. Blocks of human, monkey, pig, or mouse pancreas (0.5 cm^3) were fixed in Bouin's fixative solution (Sigma) for 4–6 h, dehydrated in 70% ethanol, and embedded in paraffin. Sections (5 μm) were cut on a microtome, air dried overnight, deparaffinized, and rehydrated. After a rinse with OptiMax Wash Buffer (Biogenex, San Ramon, CA), sections were incubated in Universal Blocker Reagent (Biogenex) for 5–10 min, rinsed again in OptiMax Wash Buffer, and incubated in Protein Block (Biogenex) for 20 min. Thereafter, sections were incubated overnight with anti-insulin (1:500, Accurate Chemical & Scientific, Wesbury, NY), anti-glucagon (1: 2,000, Sigma), anti-somatostatin (1:500, Serotec), and anti-pancreatic polypeptide (1:100, Serotec) antibodies. To visualize blood vessels, we incubated the sections in a mixture of anti-CD34 (1:500, Biogenex) and anti-smooth muscle actin (1: 2,000, Sigma) together with antisera against two of the endocrine hormones. Immunostaining was visualized by using Alexa Fluor conjugated secondary antibodies (1:400, Molecular Probes). Cell nuclei were stained with DAPI (Molecular Probes). Slides were mounted with ProLong Anti Fade (Molecular Probes) and coverslipped. As a negative control, we substituted the primary antibody with the serum of the animal used to raise this antibody. No staining was observed under these conditions. We could never see an overlap in the staining patterns for the four endocrine hormones, indicating that there was no crossreactivity between antisera and that the different immunofluorescent signals could be readily discriminated.

Data Analysis. Pancreatic sections containing islets were examined for the expression of the different endocrine and vascular markers by using a Zeiss LSM 510 scanning confocal microscope. We chose an optical section of 1 μm for all image acquisitions. All images were digitally acquired and not further processed. Sections were viewed at magnifications ×20 and ×40.

Islets (2–5 per section) were selected randomly by using the nuclear staining (DAPI) as a guide in at least three sections per pancreatic region from five human subjects and three mice. Cells were counted on digitized images, pooled from all examined sections in an individual human or mouse, and the average from all of the pancreata was calculated for each species. The proportional contribution of a cell type was calculated as the number of immunoreactive cells for that endocrine marker divided by the total number of cells immunoreactive for all of the markers. Only cells that had a clearly labeled nucleus were counted. Because we focused on pancreatic regions with few cells containing pancreatic polypeptide (<2%), we did not include these cells in the analyses. Results are expressed as mean ± SEM.

We further established whether cells contacted cells of other cell types (heterotypic associations) or cells of the same type (homotypic associations). To be counted as a contact, the edges of two cells had to be closer than 3 μm on our confocal images. Cells were included only if they had clearly visible nuclei and a strongly stained cytoplasm. These criteria were also applied to evaluate contacts between endocrine and vascular cells. The number of cells having homotypic associations, heterotypic associations, or associations with vascular cells was expressed as a percentage of the total number of that particular cell type. These values were pooled from all of the sections and averaged as described above. We further examined whether there was a particular sequence of cells aligned along blood vessels. We took advantage of the fact that at least one blood vessel per islet was cut along its main axis in our sections. Only long stretches of vessels with a visible lumen spanning a row of at least five cells were inspected. We examined vessels in 24 sections from three human subjects.

For statistical comparisons, we used one-way ANOVA, followed by Bonferroni multiple comparisons test.

$[Ca^{2+}]_i$ Imaging. Islets from human pancreata were isolated at the Human Islet Cell Processing Facility of the Cell Transplant Center at the Miller School of Medicine, University of Miami. The glands were cold-preserved in University of Wisconsin solution (27). Islets were isolated by using a modification of the automated method (28) with seven different lots of the enzyme Liberase HI (Roche) and a standard purification step, as described in ref. 28. Monkey and mouse islet isolation was performed by using modifications of the automated method for human islet isolation (28), adapted for isolation of monkey islets (29) and mouse islets (30). Human islets were dissociated into single cells by using enzyme-free cell-dissociation buffer (Invitrogen). Islets from all three species were cultured identically (37°C and 5% CO_2) in Connaught Medical Research Laboratories (CMRL) medium 1066 (Invitrogen), niacinamide (10 mM, Sigma), ITS (BD Biosciences), Zn_2SO_4 (15 μM, Sigma), Gluta

Max (Invitrogen), Hepes (25 mM, Sigma), FBS (10%, Invitrogen), and penicillin–streptomycin (Invitrogen).

For $[Ca^{2+}]_i$ imaging, islets or dispersed islet cells were immersed in Hepes-buffered solution (125 mM NaCl, 5.9 mM KCl, 2.56 mM $CaCl_2$, 1 mM $MgCl_2$, 25 mM Hepes, and 0.1% BSA, pH 7.4). Glucose was added to give a final concentration of 3 mM. Islets or dispersed islet cells were incubated in Fura 2-AM (2 μM for 1 h) and placed in a closed small-volume imaging chamber (Warner Instruments, Hamden, CT). Stimuli were applied with the bathing solution. Islets loaded with Fura 2-AM were excited alternately at 340 and 380 nm with a monochromator light source (Optoscan Monochromator, Cairn, Faversham, U.K.). Images were acquired with a Hamamatsu camera attached to a Zeiss Axiovert 200 microscope. Changes in the 340/380 fluorescence-emission ratio over time were analyzed in individual islets and dispersed cells by using the program AQM ADVANCE (Kinetic Imaging, Richmond, VA). Peak changes in the fluorescence ratio constituted the response amplitude.

We thank the members of the Human Cell Processing Facility, Translational Research Laboratory of the Cell Transplant Center, Clinical Islet Transplant Center, Organ Procurement Organizations, the Imaging Core at the Diabetes Research Institute, Administrative Offices at the Diabetes Research Institute, and Kevin Johnson for excellent technical assistance. This work was supported, in part, by National Institutes of Health Grants M01RR16587 and 1R01-DK55347-IU42RR016603 (for the General Clinical Research Center) and DK-58508, Islet Cell Resources Grant 5U42RR016603, Juvenile Diabetes Research Foundation International Grant 4-2004-361, the Diabetes Research Institute Foundation, the Swedish Research Council, the Novo Nordisk Foundation, the Swedish Diabetes Association, and the Family Stefan Persson Foundation.

1. Orci, L. & Unger, R. H. (1975) *Lancet* **2,** 1243–1244.
2. Nussey, S. S. & Whitehead, S. A. (2001) *Endocrinology: An Integrated Approach* (BIOS Scientific, Oxford, U.K.).
3. Greenspan, F. S. & Gardner, D. G. (2001) *Basic & Clinical Endocrinology* (McGraw–Hill, New York).
4. Wieczorek, G., Pospischil, A. & Perentes, E. (1998) *Exp. Toxicol. Pathol.* **50,** 151–172.
5. Stefan, Y., Orci, L., Malaisse-Lagae, F., Perrelet, A., Patel, Y. & Unger, R. H. (1982) *Diabetes* **31,** 694–700.
6. Rahier, J., Goebbels, R. M. & Henquin, J. C. (1983) *Diabetologia* **24,** 366–371.
7. Clark, A., Wells, C. A., Buley, I. D., Cruickshank, J. K., Vanhegan, R. I., Matthews, D. R., Cooper, G. J., Holman, R. R. & Turner, R. C. (1988) *Diabetes Res.* **9,** 151–159.
8. Sakuraba, H., Mizukami, H., Yagihashi, N., Wada, R., Hanyu, C. & Yagihashi, S. (2002) *Diabetologia* **45,** 85–96.
9. Street, C. N., Lakey, J. R., Shapiro, A. M., Imes, S., Rajotte, R. V., Ryan, E. A., Lyon, J. G., Kin, T., Avila, J., Tsujimura, T. & Korbutt, G. S. (2004) *Diabetes* **53,** 3107–3114.
10. Brissova, M., Fowler, M. J., Nicholson, W. E., Chu, A., Hirshberg, B., Harlan, D. M. & Powers, A. C. (2005) *J. Histochem. Cytochem.* **53,** 1087–1097.
11. Klöppel, G., In't Veld, P. A., Stamm, B. & Heitz, P. U. (1998) in *Functional Endocrine Pathology*, eds. Kovacs, K. & Asa, S. L. (Blackwell Science, Malden, MA), pp. xiv, 1138, and [8] of plates.
12. Quesada, I., Nadal, A. & Soria, B. (1999) *Diabetes* **48,** 2390–2397.
13. Santos, R. M., Rosario, L. M., Nadal, A., Garcia-Sancho, J., Soria, B. & Valdeolmillos, M. (1991) *Pflügers Arch.* **418,** 417–422.
14. Valdeolmillos, M., Santos, R. M., Contreras, D., Soria, B. & Rosario, L. M. (1989) *FEBS Lett.* **259,** 19–23.
15. Orci, L., Baetens, D., Ravazzola, M., Stefan, Y. & Malaisse-Lagae, F. (1976) *Life Sci.* **19,** 1811–1815.
16. Ichii, H., Inverardi, L., Pileggi, A., Molano, R. D., Cabrera, O., Caicedo, A., Messinger, S., Kuroda, Y., Berggren, P.-O. & Ricordi, C. (2005) *Am. J. Transplant* **5,** 1635–1645.
17. Starich, G. H., Zafirova, M., Jablenska, R., Petkov, P. & Lardinois, C. K. (1991) *Acta Histochem.* **90,** 93–101.
18. Gomez Dumm, C. L., Console, G. M., Luna, G. C., Dardenne, M. & Goya, R. G. (1995) *Pancreas* **11,** 396–401.
19. Yukawa, M., Takeuchi, T., Watanabe, T. & Kitamura, S. (1999) *Anat. Histol. Embryol.* **28,** 13–16.
20. Brelje, T. C., Scharp, D. W. & Sorenson, R. L. (1989) *Diabetes* **38,** 808–814.
21. Weir, G. C. & Bonner-Weir, S. (1990) *J. Clin. Invest.* **85,** 983–987.
22. Bonner-Weir, S. & Orci, L. (1982) *Diabetes* **31,** 883–889.
23. Stagner, J. I., Samols, E., Koerker, D. J. & Goodner, C. J. (1992) *Pancreas* **7,** 26–29.
24. Brunicardi, F. C., Stagner, J., Bonner-Weir, S., Wayland, H., Kleinman, R., Livingston, E., Guth, P., Menger, M., McCuskey, R., Intaglietta, M., *et al.* (1996) *Diabetes* **45,** 385–392.
25. Ravier, M. A., Guldenagel, M., Charollais, A., Gjinovci, A., Caille, D., Sohl, G., Wollheim, C. B., Willecke, K., Henquin, J. C. & Meda, P. (2005) *Diabetes* **54,** 1798–1807.
26. Nadal, A., Quesada, I. & Soria, B. (1999) *J. Physiol.* **517,** 85–93.
27. Kuroda, Y., Kawamura, T., Suzuki, Y., Fujiwara, H., Yamamoto, K. & Saitoh, Y. (1988) *Transplantation* **46,** 457–460.
28. Ricordi, C., Lacy, P. E., Finke, E. H., Olack, B. J. & Scharp, D. W. (1988) *Diabetes* **37,** 413–420.
29. Kenyon, N. S., Chatzipetrou, M., Masetti, M., Ranuncoli, A., Oliveira, M., Wagner, J. L., Kirk, A. D., Harlan, D. M., Burkly, L. C. & Ricordi, C. (1999) *Proc. Natl. Acad. Sci. USA* **96,** 8132–8137.
30. Berney, T., Molano, R. D., Cattan, P., Pileggi, A., Vizzardelli, C., Oliver, R., Ricordi, C. & Inverardi, L. (2001) *Transplantation* **71,** 125–132.